Proceedings of the XII International Symposium on Dynamic Problems of Mechanics (DINAME 2007), Varoto, P. S. and Trindade, M. A. (Editors), ABCM, Ilhabela, SP, Brazil, February 26 - March 2, 2007

Experimental Investigation of the Vibration Characteristics of Unmanned Aerial Vehicles

Andre Moreno da Costa Moreira [1], Leandro Ribeiro de Camargo [1], Adolfo Gomes Marto [1] , and Roberto Gil Annes da Silva [1]

[1] Instituto de Aeronáutica e Espaço – Praça Marechal do Ar Eduardo Gomes, 50 São José dos Campos, SP, Brasil

Abstract: The present work concerns the investigation of the structural dynamic behavior of Unmanned Aerial Vehicles (UAV) via experimental modal analysis. The UAV structure, named herein as, UAV airframe is composed by lightweight aluminum structure build assembling plates, beams and shells. The operational characteristics of UAVs require the qualification of the airframe regarding its aeroelastic stability and response and environmental conditions such as vibration in operation. The scope of the present investigation is the comparison of two excitation techniques for the measurement of the frequency response of the airframe, Acauã, based on mapping of airframe natural mode shapes and frequencies. The first method of excitation employs an electro-dynamic shaker to randomly excite the airframe in a single reference position in the structure in a limited frequency range. The second method is based in the impulsive excitation of the airframe using an impact hammer at the same structural position where the electro-dynamic shaker was set. The results of the present investigation indicate the advantages and drawback regarding using each of these two distinct excitation techniques for the excitation of this class of lightweight structure.

Keywords: Unmanned aerial vehicle, modal analysis, mode shape

NOMENCLATURE

A	residues corresponding to the mode shape
$\mathbf{D}$	damping coefficients matrix
F	generalized force vector in time domain
F	generalized force vector in frequency domain
$\mathbf{F}$	generalized force vector in time domain
FRF	Frequency Response Function
h	impulse response of system in time domain
H_v	FRF estimator
i	imaginary number $\sqrt{-1}$
$\mathbf{I}$	Indentity matrix
$\mathbf{K}$	stiffness matrix
$\mathbf{M}$	mass matrix
MSCC	Mode Shape Correlation Coefficient
PRCE	Poly-Reference Complex Exponential method
q	generalized coordinates vector in time domain
Q	generalized coordinates vector in frequency domain
S	Laplace variable
S_{kk}, S_{ii}	force and response auto-spectra, respectively
V_r	$e^{s_r \Delta t}$ diagonal matrix
UAV	Unmanned Aerial Vehicle
W	relationship between the residues and the first residue
X, Y, Z	orthogonal coordinate system axis

Greek symbols

α	receptance in frequency domain
Φ	natural mode shape normalized by mass matrix $\mathbf{M}$
Φ_h	natural mode shape extracted using hammer excitation.
Φ_s	natural mode shape extracted using shaker excitation.
γ^2	coherence function
ω	angular frequency
ξ	modal damping coefficient

Subscripts

r	relative to a mode shape
i	relative to output signal
k	relative to input signal
h	relative to the hammer test
s	relative to the shaker test

Superscript

*	complex conjugated
T	transpose matrix or vector

INTRODUCTION

The unmanned aerial vehicle (UAV) technology, have been developed to replace the employment of conventional aircraft in many kinds of risk operations regarding safety (no human lives involved), and also low cost, as commented by Blyenburgh (1999) and Herrick (2000). Among the risk operations, this kind of aircraft may be used in the military operations. A special kind of military operation is the artillery training using such unmanned vehicles. This vehicle is also known as "drone" due to a target mark in the tail, like a drone. Another utilization of this class of aircraft is its employment as a tactical surveillance system.

These aircraft are remotely or auto-piloted vehicles. The missions to be accomplished could be pre-programmed as a prescribed flight path to attend a desired operation. For this reason, its guidance and navigation system includes an autopilot, which consists in a control system implemented to pilot the UAV along the desired flight path. Furthermore, it would be desirable to have robust flight control system laws designed for a well identified dynamic system. The reader should conclude that the flight of an UAV could be very sensitive to atmospheric disturbances, and its auto-piloting system must be sufficiently accurate to take into account aeroelastic response due such environmental conditions

The autopilot control system can be understood as a dynamic system interacting with the dynamics and aerodynamics of the UAV. Thus, it would be desirable the best knowledge of the structural dynamic behavior of this airframe, including the stability of the system caused by any flight parameter variation. In other words, it is necessary to be sure that the airframe is free of aeroelastic instabilities such as flutter.

In the case of UAVs employed as sensorcrafts, that is, its main task is sensoring, the accuracy of the data acquisition systems strongly depends on environmental conditions. One cause of the lost of accuracy of the sensoring systems is closely related to how does the aircraft vibrates at certain airframe locations. This care need also to be taken to circumvent any possible mechanical disturbances in the electronic devices installed in the aircraft, which could compromise the operation of the sensoring systems.

The main objective of the present investigation is to be sure that the experimental modal model is sufficiently accurate for the update of a finite element structural dynamic model. For this reason, two excitation methods for experimental modal analysis are used to verify which of them is best suited for the present application.

When the reader looks for information on experimental modal analysis for small or lightweight structures, the excitation, in most of the cases, is performed by the use of impact hammers. However, such kind of excitation could not be the best one for the experimental modal analysis of a given structure, as indicated by Corelli and Brown (1984). These authors pointed out several drawbacks regarding this methodology. However, Corelli and Brown (1984) also indicate that the impact testing is fast, easy and portable. These features are very convenient in the cases of demanding applications such the UAVs structural preliminary design and sensors installation phases.

Both excitation techniques where applied for the experimental modal analysis of the chosen test bed the Acauã UAV. The modal characteristics and the correlation between the two excitation methods are presented in the results allowing the authors to conclude which method is the best suited for the modal surveillance of this class of vehicles.

TEST SETUP

The airframe, the points where the accelerometers are positioned, as well as the exciters are illustrated squematically in the Fig 1:

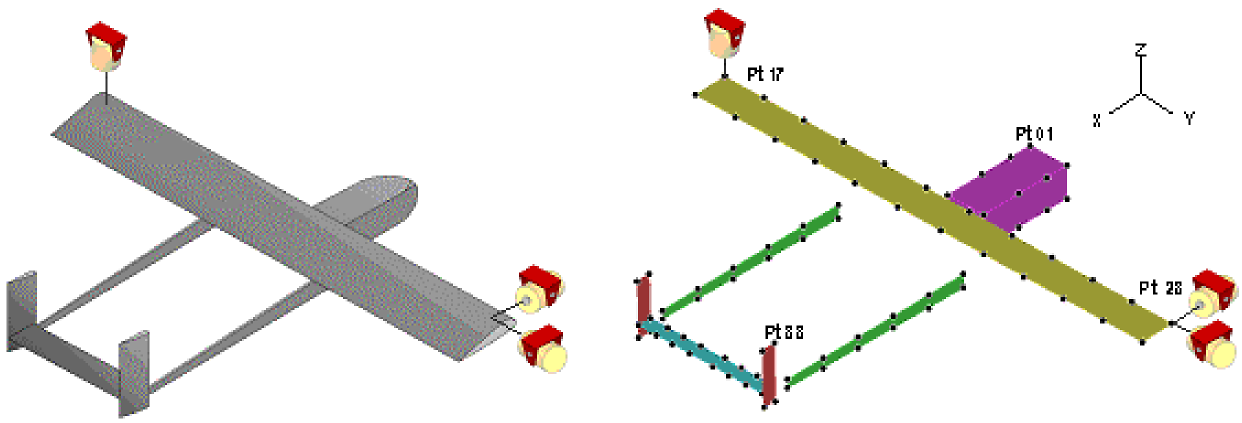

Figure 1 – Schematic illustration of accelerometer and exciters positions

Once the objective of this investigation is to compare both kind of excitation, e.g, electrodynamic shaker and impact hammer, it was chosen the same point for the application of the exciting forces. As one can observe in the Fig 1, the point 28 is chosen to excite the airframe in the X and Y directions and the point 17 to excite in the Z direction. The data acquisition and signal processing parameters settled in the acquisition system for both tests are presented in the Tab 1. Although the range of frequency analysis was chosen between 0 and 128 Hz, only results regarding the identified modal parameters (frequency, damping and mode shapes) within the 0 to 60 Hz band is, in the aeroelasticity point of view, of interest. This is so because, for aeroelastic applications, the structural dynamic numerical model and the identified modal parameters must be well correlated once the aeroelastic behavior of the airframe strongly depends on the dynamic model of the system.

Table 1 – Signal processing parameters.

Parameters	Shaker	Hammer
Analysis frequency (Hz)	128	128
Frequency resolution (Hz)	0.0625	0.250
Average type	Stable	Stable
Number of averages	80	7
Spectral analysis window	Hanning	Force/Exponential

GENERAL MATHEMATICAL BACKGROUND

The displacements occurring on the structure can be mathematically described in terms of the generalized coordinates *q(t)*. Applying the Lagrange and Hamilton principles to this generalized coordinates we obtain the equation of motion:

$$\mathbf{M}\,\ddot{q} + \mathbf{D}\,\dot{q} + \mathbf{K}\,q = \mathbf{F}(t) \quad , \tag{1}$$

where **M**, **D** and **K** are the generalized mass, damping and stiffness matrices, respectively. **F** is the generalized force vector. In the frequency domain the equation of motion becomes:

$$\left(-\omega^2\,\mathbf{M} + \mathrm{i}\,\omega\mathbf{D} + \mathbf{K}\right) Q(\omega) = F(\omega) \quad . \tag{2}$$

The information about the dynamic characteristics of the system can be described as the receptance (α) relationship:

$$\alpha(\omega) = \frac{X(\omega)}{F(\omega)} = \left(-\omega^2\,\mathbf{M} + \mathrm{i}\,\omega\mathbf{D} + \mathbf{K}\right)^{-1} \tag{3}$$

where each matrix coefficient α_{jk} corresponds to one frequency response function, describing the relation between a particular response in the coordinate *j* due to a particular force applied in coordinate *k*. Using the modal properties of a linear non-damped system, with the natural mode shape normalized by mass matrix **M** the following relations are valid:

$$\Phi^T\,\mathbf{M}\,\Phi = \mathbf{I} \quad \text{and} \quad \Phi^T\,\mathbf{K}\,\Phi = \left\lfloor \diagdown \omega_r^{\,2} \diagdown \right\rfloor \quad , \tag{4}$$

and the FRF of each element can be written as

$$\alpha_{jk}(\omega) = \sum_{r=1}^{N} \left(\frac{{}_rA_{jk}}{\omega_r\xi_r + \mathrm{i}\left(\omega - \omega_r\sqrt{1-\xi_r^2}\right)} + \frac{{}_rA_{jk}^{\;*}}{\omega_r\xi_r + \mathrm{i}\left(\omega - \omega_r\sqrt{1-\xi_r^2}\right)} \right), \tag{5}$$

where ${}_rA_{jk}={}_r\Phi_j\ {}_r\Phi_k$ are the residues corresponding to the mode shape *r*, with natural frequency ω_r and modal damping coefficient ξ_r. Applying frequency domain digital signal processing techniques, the FRFs can be estimated experimentally, as in Rocklin et al (1985),

$$\alpha_{jk} \cong H_v = \sqrt{\frac{S_{kk}(\omega)}{S_{jj}(\omega)}} \tag{6}$$

where, S_{kk} is the auto-spectra of the signal of the force, S_{jj} is the auto-spectra of the signal of the accelerometer in the point *j*, both calculated by a Fast Fourier Transform Algorithm. The coherency γ^2 is computed in order to evaluate the quality of the signal with respect at the presence of interference noise among the measurements.

$$\gamma_{jk}^2(\omega) = \frac{\left|S_{jk}(\omega)\right|^2}{S_{jj}(\omega)\,S_{kk}(\omega)} \qquad 0 \le \gamma_{jk}^2(\omega) \le 1 \tag{7}$$

Although the FRFs had been calculated with only one force reference individually, it was employed a multiple input multiple output method (MIMO), using all reference used in order to extract the dynamic characteristic. The chosen method was Polyreference Exponential Complex Method, PRCE, described in detail in Vold and Roklin (1982). The impulse response of system is calculated using the Inverse Fourier Transform of the FRFs:

$$h_{jk}(t) = \sum {}_rA_{jk}\, \mathrm{e}^{s_r t} \ , \tag{8}$$

where

$$s_r = -\omega_r \xi_r + i\omega_r \sqrt{\left(1-\xi^2\right)} \ . \tag{9}$$

Considering that the residues ${}_rA_{jk}$ relate with the first residue ${}_rA_{j1}$ by

$${}_rW_{k1} = \frac{\psi_{kr}}{\psi_{1r}} , \tag{10}$$

the Eq. (8) can be written for *n* input reference point in form of matrix

$$\left\{h_j(t)\right\} = [W] \begin{bmatrix} e^{s_1 t} & 0 & \cdots & 0 \\ 0 & e^{s_2 t} & \cdots & 0 \\ \vdots & \vdots & \ddots & \vdots \\ 0 & 0 & \cdots & e^{s_{2N} t} \end{bmatrix} \left\{A_{j1}\right\} = [W][V_r]\left\{A_{j1}\right\} \tag{11}$$

The coefficients of V_r are calculated using Prony´s method, consequently the natural frequencies, modal damping coefficients, and also the *W* values. Finally the residues can be computed from the experimental data.

Two different excitation methods where used to excite the structure. One random using an electrodynamic shaker limited in a frequency band, the other is impulsive using the dynamometric hammer. The coherencies and reciprocities of FRFs signals are analyzed using both excitation techniques and compared between each other. The correlation between the modes extracted from the random excitation and the mode extracted from the impulse excitation are calculated using “Mode Shape Correlation Coefficient” written in Ewins (1984), and given by:

$$MSCC(h,s)=\frac{\left|\sum_{r=1}^{n}(\Phi_h)_r(\Phi_s)_r^*\right|^2}{\left(\sum_{r=1}^{n}(\Phi_h)_r(\Phi_h)_r^*\right)\left(\sum_{r=1}^{n}(\Phi_s)_r(\Phi_s)_r^*\right)} \tag{12}$$

where Φ_h are the modes resulted from hammer excitation method and Φ_s are modes computed from the electrodynamic shaker method. When the computed modes shapes vectors corresponding to a given natural frequency correlate between each other, the corresponding MSCC matrix coefficient approximate to the unit value. In the other case, when the modes are uncorrelated the corresponding MSCC matrix coefficient approach zero. The mathematical significance of the MSCC coefficients is based on the idea of quantifying the orthogonality level between two distinct eigenvectors under comparison.

RESULTS

Each test has used 792 FRFs in order to estimate the airframe modal parameters. Only results obtained from driving points are presented in this paper. The FRFs and coherence comparison extracted on axis X, Y and Z are shown on the Fig 2, Fig 3, and Fig 4.

The modal parameters are extracted using the CADA-X^{TM} dynamic data processing software, using the PRCE method. The stiffness was normalized by mass matrix **M**. Table 2 presents the identified modal parameters within the frequency range of interest (0 to 60 Hz) for comparison. The first six structural mode shapes are presented in the Fig 5.

Another investigation to be performed concerns the reciprocity analysis. For both excitation methods, the shaker reciprocity analysis is presented in the Fig 6 and using the analysis for the impact hammer case in the Fig 7.

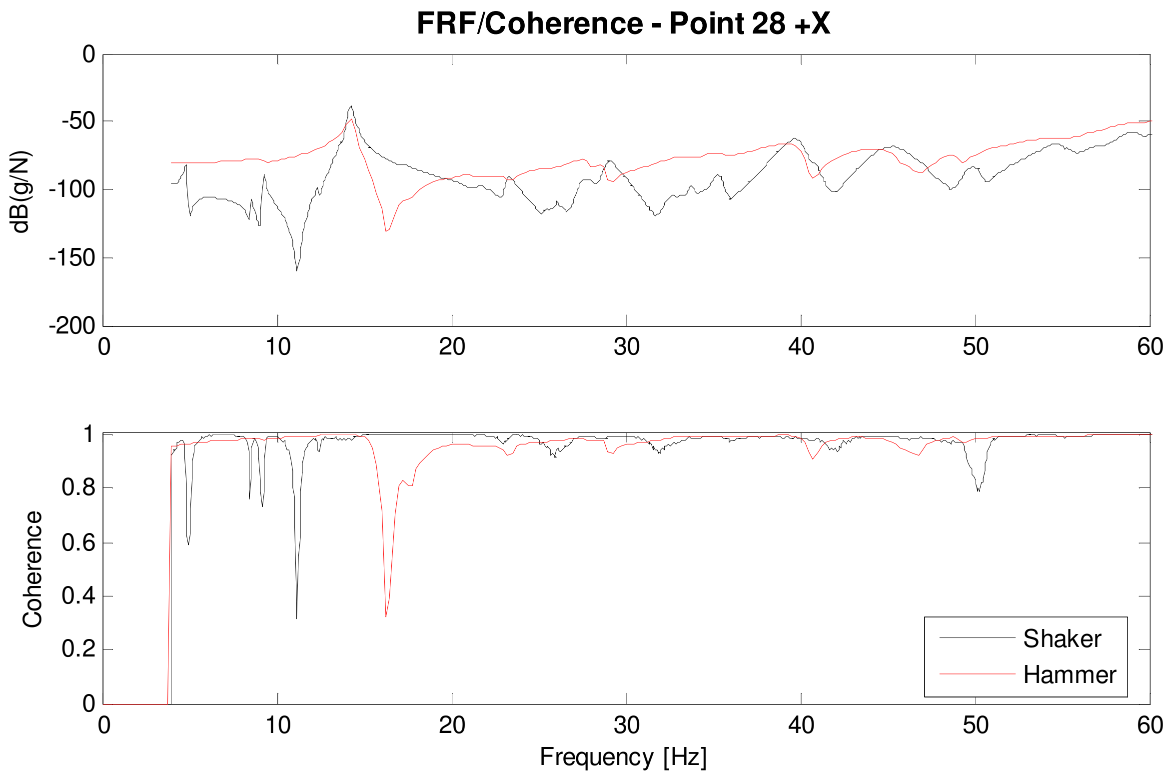

Figura 2 – FRFs and coherences of driving point 28 in X direction.

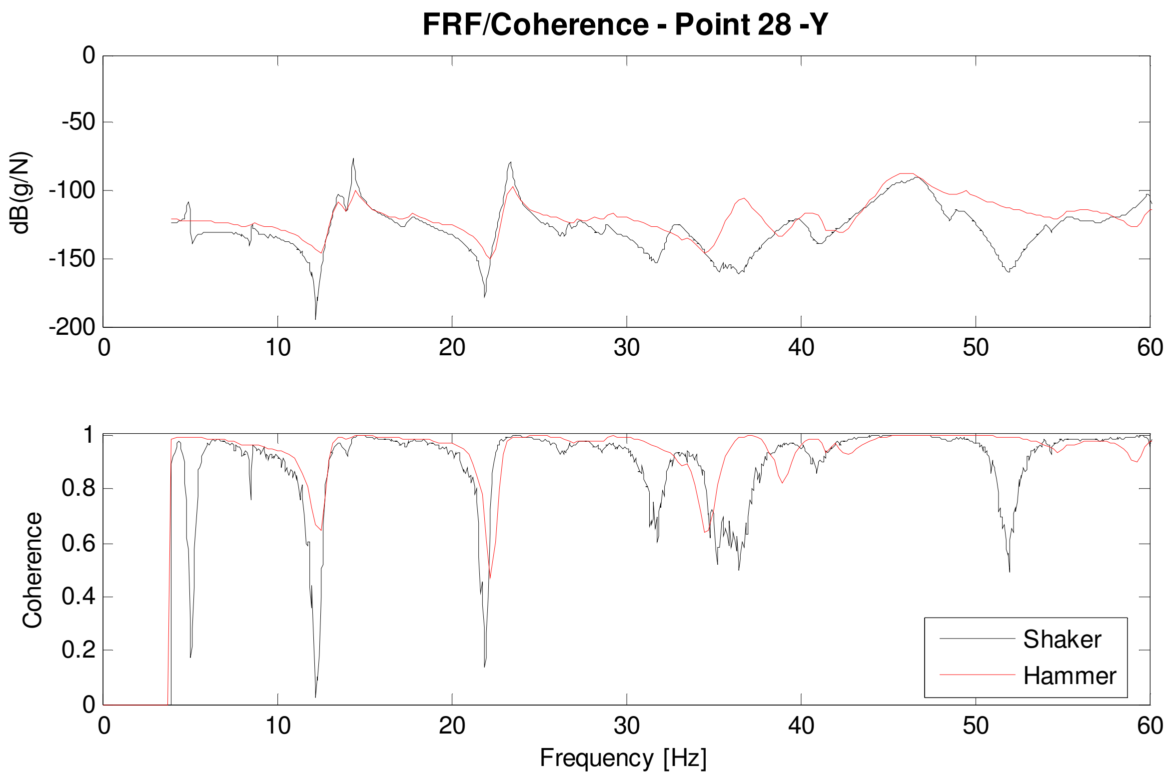

Figura 3 – FRFs and coherences of driving point 28 in Y direction.

The modes obtained by impulsive excitation and random excitation have been correlated using the MSSC implemented in MalabTM. Table 3 presents the results of the correlations analysis, and as one can observe, a good correlation between the modes resulted from the shaker and impact hammer was achieved.

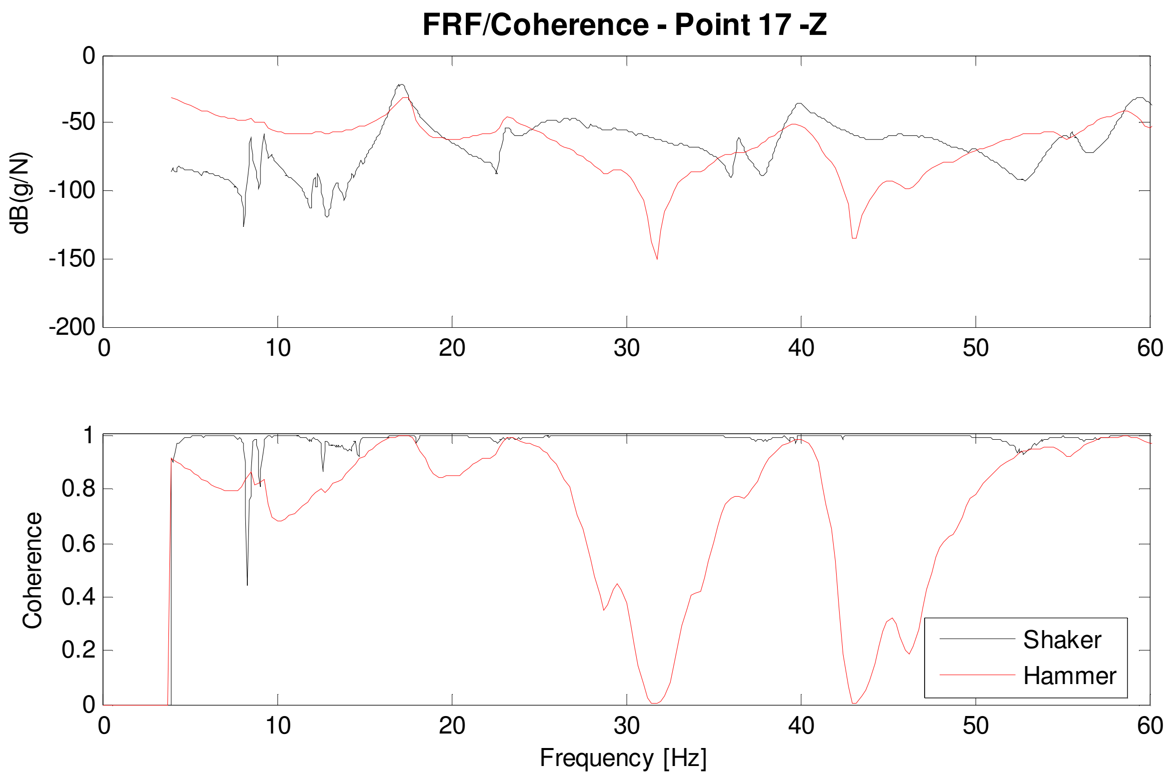

Figure 4 – FRFs and coherences of driving point 17 in z direction.

Table 2 – Comparison of generalized modal parameters

Mode	Random Excitation (Shaker)			Impulsive Excitation (Hammer)		
	Frequency (Hz)	Damping (%)	Stifness (N/m)	Frequency(Hz)	Damping(%)	Stifness(N/m)
1	8.51	0.82	2859	8.56	1.01	2894
2	9.26	0.84	3387	9.26	0.74	3385
3	14.34	0.52	8120	14.28	0.59	8052
4	17.22	1.96	11716	17.54	1.98	12152
5	21.51	1.37	18263	-	-	-
6	23.56	1.00	21354	23.23	0.98	21297
7	29.62	1.23	34652	27.64	0.76	30171
8	33.71	0.90	44878	33.50	1.01	44307
9	36.43	0.51	52386	35.69	0.79	50289
10	40.05	1.34	63325	39.72	2.35	62329
11	45.18	1.90	80614	-	-	-
12	46.57	0.68	85643	-	-	-
13	48.99	1.96	94746	48.88	0.64	94321
14	56.19	0.87	124690	54.90	1.18	119010

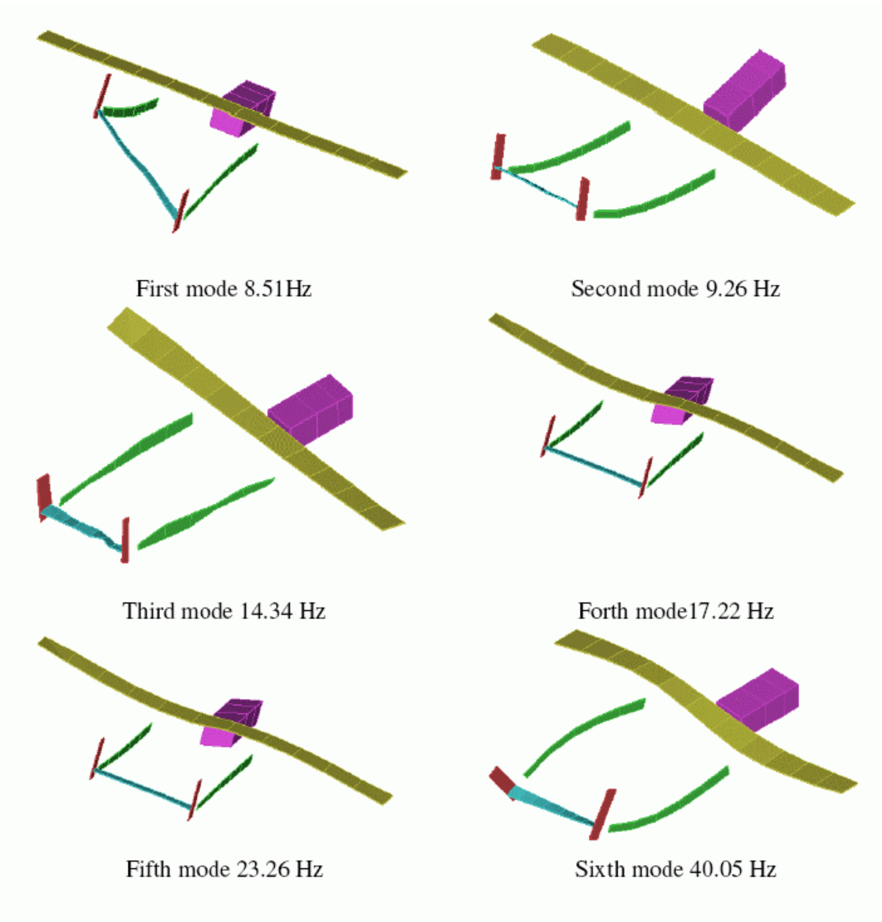

Figure 5 Natural modes of Acauã airframe.

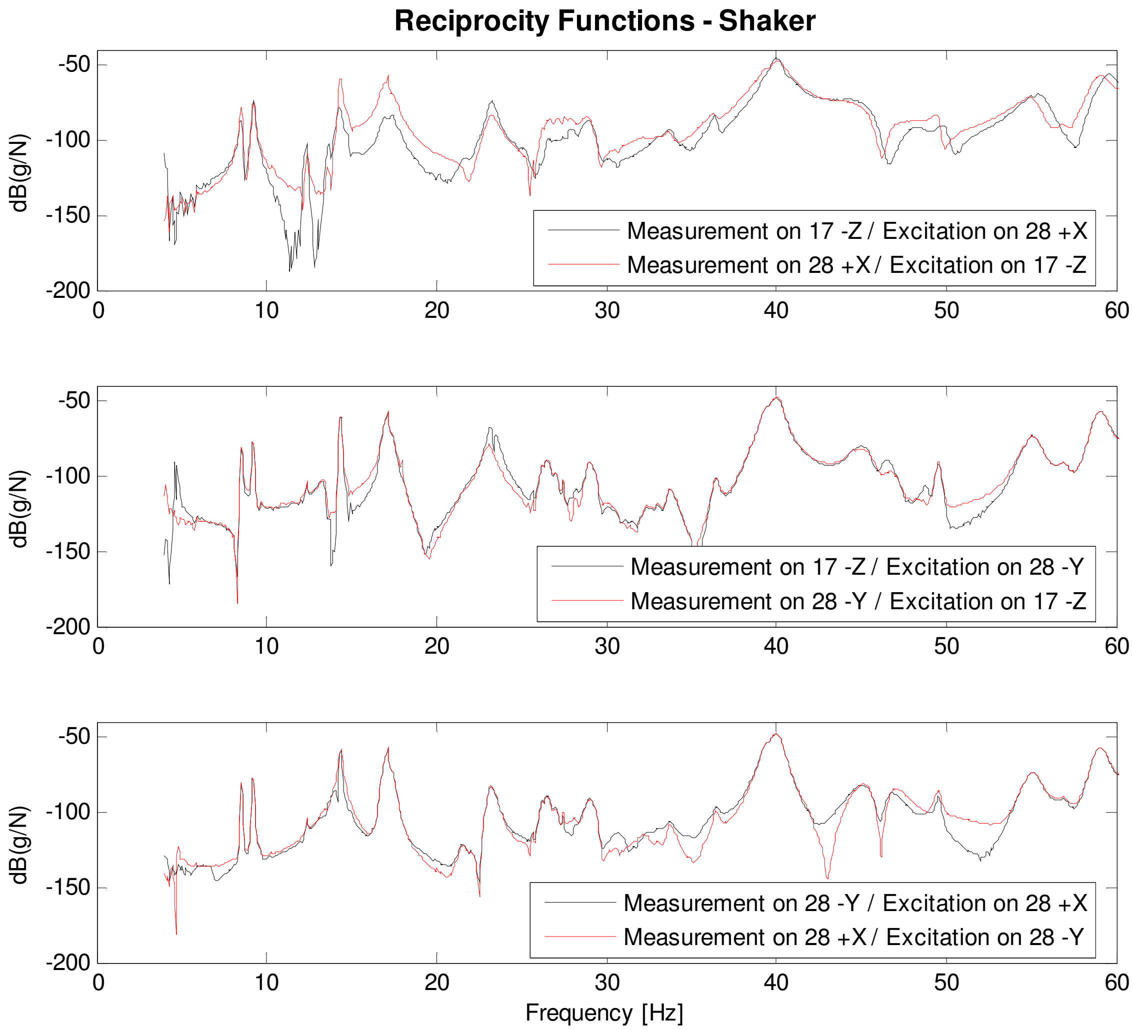

Figure 6 Comparison reciprocity when the strucuture is excited by shaker

Table 3 Mode Correlation between modes obtained via impulsive and random excitation

	Impulsive		Random	
MSCC No.	**Mode no.**	**Frequency (Hz)**	**Mode no.**	**Frequency (Hz)**
0.9323	1	8.5617	1	8.5106
0.9125	2	9.2608	2	9.2627
0.9345	4	17.5413	4	17.2241
0.8765	5	23.2738	6	23.2572
0.8068	7	33.4993	8	33.7148
0.7150	7	33.4993	9	36.4269
0.7861	9	39.7232	10	40.0468
0.8407	10	48.8783	13	48.9881
0.8876	11	54.9013	14	56.1898
0.7219	13	70.4365	17	70.3916

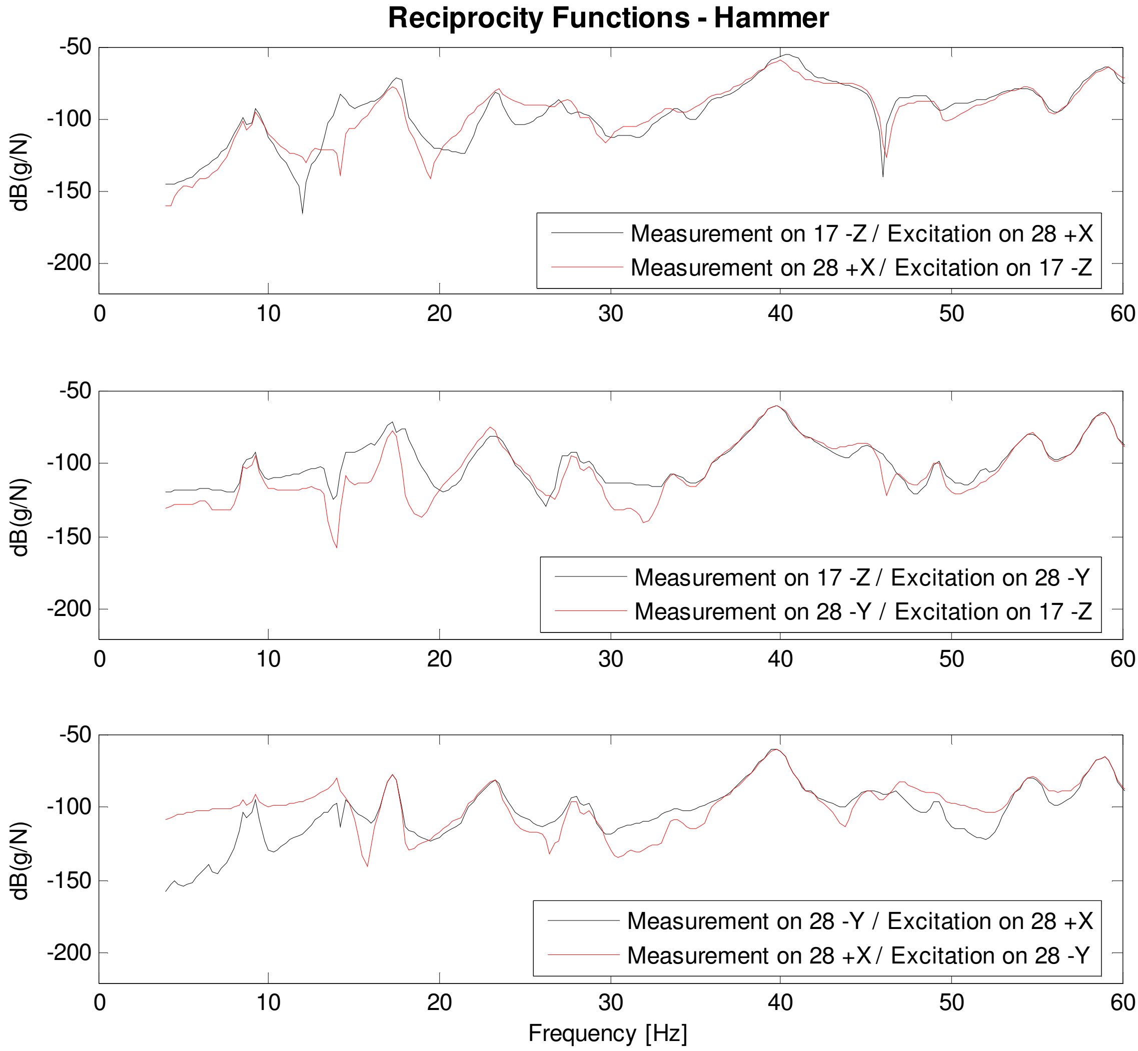

Figure 7 Comparison reciprocity when the strucuture is excited by hammer

CONCLUSION AND REMARKS

The scope of the present work is to provide conditions for the choice of the best excitation technique for the modal test, evaluating the cost-benefit relation when timeframe and accuracy are compromised.

The investigation indicates that both excitation methods present good results considering the identification of the structural dynamic behavior of the airframe under analysis. The frequency and modal damping agreed well. Three of the identified model shapes using the electrodynamic shaker method were not captured when using the impact hammer. The explanation for this discrepancy is because the utilization of the impact hammer to excite the whole airframe does not provide sufficient energy for the excitation of certain natural mode shapes.

A possible way to circumvent such deficiency is to change the position of the excitation point. However, the scope of the present investigation is to compare two excitation methods. Thus, a change of excitation point for the impact hammer test does not make sense, because an issue to be evaluated is the capability of the energy transfer along the airframe using both methods of excitation. So, the setting of a common excitation point is our reference to compare these two methodologies.

The fact of uncorrelated modes and also non-captured mode shapes reinforce the idea that the impulsive excitation is not sufficient for medium-sized airframe. In the case of Acauã UAV, it was concluded that there was not available energy to excite all modes of interest, when the excitation of its structure was performed using the impact hammer.

Another result to be considered is the reciprocities represented in Fig 6 and 7. One should observe that both excitation methods provide sufficient reciprocity indicating that the airframe presents a linear behavior within the frequency and force level excitation ranges.

Looking at the results using both excitation procedures, it is also possible to conclude that the mode shapes are well correlated, when both excitation methods are quantitatively compared when the mode correlation coefficients are computed.

This work was a first stage of a structural model conception in order to represent this dynamic characteristic. A Finite Element Model will allow to investigate the airframe behavior with others parts, as well as the aeroelastic stability in flight condition.

ACKNOWLEDGMENTS

The authors would like to acknowledge Fundação Casimiro Montenegro for supporting this research.

REFERENCES

Corelli, D. and Brown, D.L. , 1984, “Impact Testing Consideration”, proceedengs of the 2nd International Modal Analysis Conference, Orlando, USA, pp. 735-742.

Cox, T.H. and Gilyard, G. B. (1986) “Ground vibration test for drones for Aerodynamic and strucutral testing (DAST)/ Aeroelastic Research Wing (ARW-1R) Aircraft”. NasaTechnical Memorandum 85906,

Ewins, D. J., 1984, “Modal Testing: Theory, Practice and Application”, Research Studies Press, Letchworth, England, 269 p.

Herrick, K., 2000, “Developed of the Unmannded Aerial Vehicle Market: Forecast and Trends”, Air & Europe Vol. 2 n.2 pp 25-27.

Maia, N. M. M., Silva, J. M. M., He, J., Lieven, N. A. J., Lin, R. M., Skingle, G. W., To, W.-M., and Urgueira, A. P. V., 1997, “Theoretical and Experimental Modal Analysis”, Research Studies Press, Taunton, England, 468p.

Rocklin, G.T., Crowley, J., Vold, H., 1985 “A. Comparison of H1, H2 and HV Frequency Response. Functions”, Proceeding of 3rd International Modal Analysis Conference, pp. 272-278

Vold, H.; Rocklin, G.T., 1982; "The Numerical Implementation of a Multi-Input Modal Estimation Method for Mini-Computers", Proceedings of International Modal Analysis Conference, Orlando, USA, pp. 542-548.

RESPONSIBILITY NOTICE